FINITE ELEMENT ANALYSIS OF DEFORMATION OF CONTAINERS WITH RADIOACTIVE MATERIALS IN EMERGENCY SITUATIONS

V. Bazhenov(1), A. Kibetz(1), Yu. Kibetz(1),
V. Matveyev(2), A. Uchayev(2)

(1) Research Institute of Mechanics, Nizhny Novgorod State University,
N.Novgorod, Russia
(2) All-Russian Scientific Research Institute of Experimental Physics,
Sarov, Russia

SUMMARY

The results of numerically analysing the behaviour of storage and transportation containers for radioactive materials under shock effects are presented. Separately analysed is the nonstationary deformation of the supporting structure (bottom plate) to which several containers are fastened for transportation.

INTRODUCTION

The report addresses 3-D problems of nonstationary elastoplastic shock deformation of structures made up of solid and shell elements. The motion of the structure is described in Lagrange variables. Relations of the theory of yielding with kinematic and isotropic hardening are used as equations of state. Contact interaction between the individual structural elements and their interaction with other bodies is modelled as rigid adhesion or one-way connection conditions allowing for sliding along a tangent plane to the contact surface and for breaking the contact. The problem is analysed using a finite element method and an explicit "cross"-type finite-difference time-integration scheme [Bazhenov and Kibetz, 1994]. The resulting family of 8-node finite elements introduced in the paper allows one to describe dynamic processes in plates and shells, using one layer of the elements through the thickness, and those in thick-walled and solid structures, using a greater number of layers. Some algorithms implementing contact interaction between deformed bodies on mismatching FE meshes are given in [Bazhenov et al.,1995]. The problems were analysed using the DINAMIKA-3 applied package.

COMPUTATIONAL RESULTS AND DISCUSSION

The container analysed is an axisymmetrical shell structure (Fig.1) consisting of (1) a body - a cylindrical shell (R=22 cm, L=80 cm, h=0.3 cm) reinforced by flange Φ_1, and (2) bottoms S_1 and S_2 - segments of a spherical shell (R=50 cm, h=0,3 cm). The container houses loads M_1, M_2 and M_3 having the masses of 16, 19 and 66 kg, respectively. Along the length of L=10.4cm adjacent to bottom S_2, the body is reinforced by a 0.3 cm thick cylindrical shell. The container is made of an aluminium alloy having the following mechanical characteristics: density ρ=2.64 g/cm^3, shear modulus G=26.1 GPa, volume compression coefficient K=56.6 GPa, yield strength σ_5=0.16 GPa, kinematic hardening modulus g_k=0.44 GPa. Slab P_1 with the mass of 500 kg falls upon the container resting on a stationary slab, P_2. Loads M_1, M_2, M_3 and slabs P_1, P_2 are modelled as linearly elastic bodies and also covered with FE-meshes. The complete FE mesh of the analysed region has 1326 finite elements. Several versions of the problem were analysed, differing in the spatial position of the container and the height from which the slab falls.

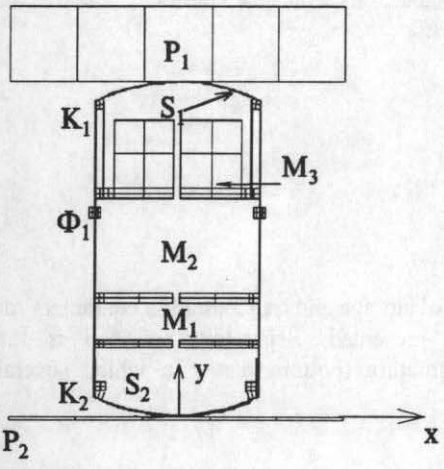

Fig. 1

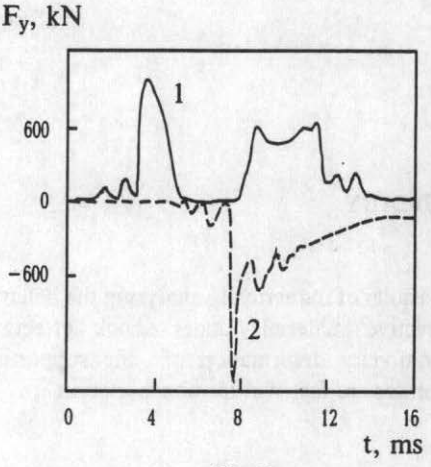

Fig. 2

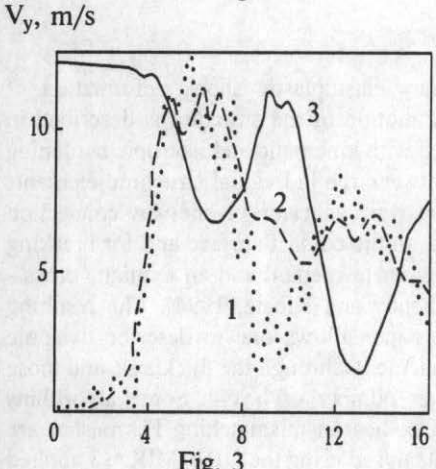

Fig. 3

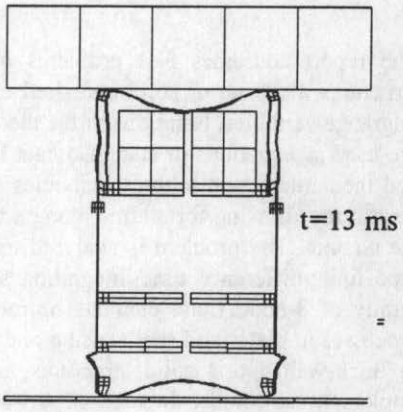

Fig. 4

In the first version, deformation of a vertical container when struck by a slab falling from the height of h=9 m was analysed. The initial velocity determined using the expression $V=(2\bar{g}h)^{1/2}$ is 13.3 m/s ($\bar{g}$=9.8 m/s^2 is gravity acceleration). The results of the analysis for this initial velocity value are summarised in Figs.2-4. Fig.2 shows time histories for contact force F_y between the falling plate, P_1, and the cover, S_1 (curve 1), the base slab, P_2, and the bottom, S_2 (curve 2). The curves in Fig.3 reflect time variation (during time t) of the vertical component of the velocity, V_y, for mass M_1 (curve 1), mass M_3 (curve 2) and slab P_1 (curve 3). Fig.4 depicts a deformed cross-section of the analysed region in the xy-plane for time t=13 ms. It is evident from the results in Figs.2-4 that, under longitudinal loading, the container deforms in three stages.

At the initial stage (up to 3 ms), deformation of the cover, S_1, occurs. Under the effect of contact pressure, the shell deflects along the Y-axis. Velocity V_y of the central portion of the shell reaches the value that exceeds the velocity of the slab, thus transforming the contact region from a round spot into a ring. As shell S_1 deforms, the radius of the ring increases, and so does the contact force value (Fig.2). As deformation of the shell is accompanied by the propagation of compression and unloading waves along the container and by their interaction, the increase of the contact force has an oscillating character. Cover S_1 being shallow and thin, the velocity of slab P_1 is reduced only marginally.

The second stage begins at t=3 ms and takes up to 6 ms. By that time the contact region between slab P_1 and the container is shifted onto attachment unit K_1, leading to a sharp increase of both the contact force in the region of interaction between slab P_1 and cover S_1 (Fig.2) and the motion velocity of masses M_1, M_2 and M_3 (the time histories of the vertical components for M_1 and M_2 practically coincide). As is evident from Fig.3, the velocity of masses M_1-M_3 on the time interval from 3.2 ms to 4.8 ms increased to 9.5 m/s. Acceleration $\Delta V/\Delta t$ of the loads on that interval is around 600 $\bar{g}$. Deceleration of slab P_1 is retarded, which is connected with the run of the stress wave along the cylindrical shell, and is not so quick, as the slab mass is an order higher than mass M_3. As a result of the deceleration of slab P_1, its contact with the container is temporally interrupted. After passing through the cylindrical shell, the stress waves set bottom S_2 in motion, leading to its contact with the stationary plate, P_2 (Fig.2, curve 2).

The third stage starts when the lower contact zone, S_2-P_2, is shifted to attachment unit K_2 and the base of the cylindrical shell. It occurs at t=7 ms and, as follows from Fig2., is accompanied by a sharp increase of the integral contact force in the S_2-P_2 region. With some delay, determined by the run length of the compression wave along the cylindrical shell of the body, the incident plate, P_1, and the upper cover, S_1, regain contact. Comparison of the curves in Fig.2 shows that, at the beginning of the third stage, contact force F_y in the lower part of the structure, S_2-P_2, is higher than in its upper part, S_1-P_1. This is due to the effect of the structure mass on the contact force value. Increase of the contact force in zone S_2-P_2 leads to the deceleration of masses M_1-M_3. The higher mass (M_3) decelerates slower, thus suffering lower overloading (Fig.3): for loads M_1 and M_3, overloading $\Delta V/\Delta t$ is 400 $\bar{g}$ and 130 $\bar{g}$, respectively. The effect of the compression loads leads to the buckling of the cylindrical shell

in the regions adjacent to the contact zones (Fig.4). This process is accompanied by a gradual decrease of contact pressure in the lower zone, S_2-P_2, and a temporary breakage of contact in the upper part (Fig.2). As is evident from Fig.4, the most intensive buckling of the cylindrical shell occurs in the region between mass M_1 and attachment unit K_2, where a fold forms finally. At t=13 ms, plastic strain intensity in the region of the fold reaches 22%. At that time, slab P_1 and loads M_1-M_3 have a considerable velocity (Fig.3). The kinetic energy of the "slab P_1 + container" system has retained 40% of its initial value. Based on this, further increase of the strain in the region of the fold can be predicted, leading to possible disintegration of the container body.

Reducing the height from which slab P_1 falls from 9 m to 4.5 m does not change qualitatively the motion of masses M_1-M_3. However, the kinetic energy value that slab P_1 acquires when falling from the height of 4.5 m is not enough for a fold to form and for the cylindrical shell to lose its stability in the region between mass M_1 and attachment K_2. The analysis of plastic strain distribution over the container body shows that their maximum values do not exceed 10%. At t=18 ms, the velocity of slab P_1 is reversed and the contact is finally lost.

The deformation of the container when struck by slab P_1 falling from the height of 4.5 m was analysed. The angle between the axis of revolution of the container in the initial position and a normal to the surface of plate P_2 was assumed to be 30 degrees. The numerical analysis results for the above problem are summarised in Figs.5-8. Fig.5 shows time histories for the vertical component, F_y, of the integral contact force. Here, the force at the falling slab is marked by 1 and that at base P_2 is marked by 2. The curves in Fig.6 depict time histories of the vertical velocity component V_y of masses M_1, M_3 (curves 1, 2) and of slab P_1 (curve 3). Figure 7 presents the cross-section geometry of the container in the symmetry plane at time t=15 ms; the FE mesh of the container is shown in Fig.8 at t=10 ms.

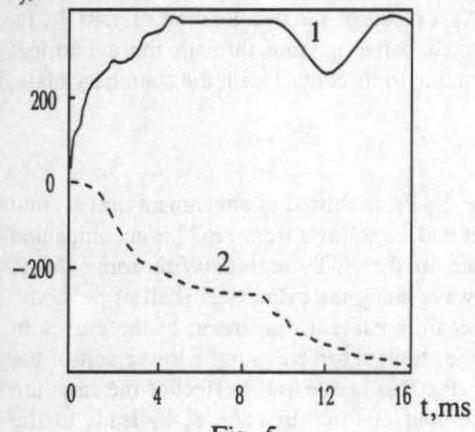

Fig. 5

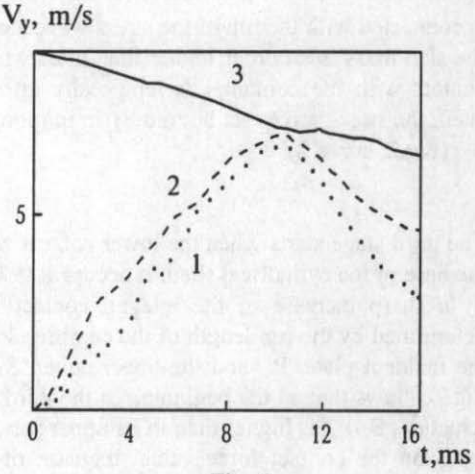

Fig. 6

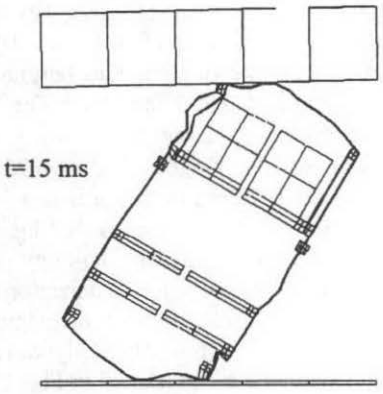

Fig. 7

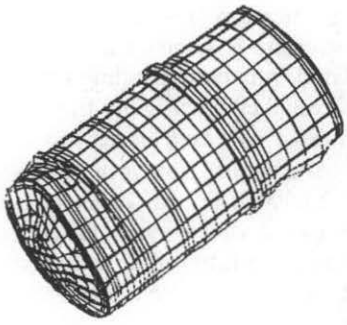

Fig. 8

It is evident that the deformational process of the container differs from that in the previous version of the problem: as slab P_1 comes in contact with the carrying structure (the cylindrical shell) from the very beginning, contact force F_y steadily increases up to 90 kN. After the loading wave has passed along the cylinder shell and reached the opposite bottom, the container comes in contact with base P_2. As the compression proceeds, nonsymmetrical local folding zones appear, first in the upper part of the container adjoining slab P_1, and then in its lower part, in the vicinity of the P_2-S_2 contact area. Some of the kinetic energy of slab P_1 is spent to form a fold, thus, limiting the level of contact pressure (Fig.5). As is evident from the curves in Fig.6, masses M_1-M_3 do not suffer significant overloading. Thus, the average acceleration value during the period from 0 to 7 ms is about $100\,\overline{g}$. However, the maximum plastic strain level for an inclined container is considerably higher than in the previous version of the problem, the plastic strain value in the vicinity of the fold at time t=10 ms reaching 28%. Thus, it can be concluded that the deflection of the axis of revolution of the container from a normal to the surface of the obstacle by 30 degrees increases the risk of its depressurization.

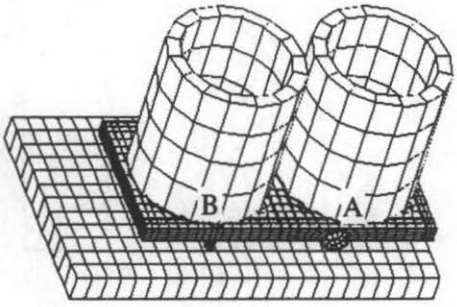

Fig. 9

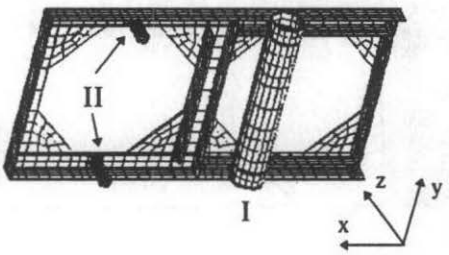

Fig. 10

When being stored or transported, containers may be secured on some supporting structure, the deformability of which is to be also taken into account. Shown below are the results of

deformation analyses of the bottom plate with 4 containers secured on it (Figs.9, 10). All of the structure is symmetrical relative to the yz-plane, thus, only one half of it ($x \geq 0$) was analysed, with corresponding symmetry conditions assigned in the yz-plane. The bottom plate is a 75x300 cm rectangular frame having vertical walls 7cm high and 0.7cm thick. The frame has tubular rails for a loader, I (R=6 cm, h=0.5cm), and posts, II (R=3 cm, h=0.6 cm), 13.6 cm high. The bottom plate is made of steel (ρ=7.8 g/cm^3, G=80 GPa, K=205 GPa, σ_s=0.25 GPa, g_k=0.2 GPa). The body of the container is a cylindrical shell, 70 cm in diameter and 75 cm high, closed with bottoms on both ends. The mass of the filled container is 247 kg. Each container is positioned on the bottom plate and secured to it with its lower bottom by planks which are bolted to the frame. In the analysis, the containers were modelled as nondeformable bodies, their attachment to the frame being approximated by rigid adhesion. At the moment of impact, the fall velocity of the bottom plate was assigned to be 13.3 m/s. The analysed region was divided into 2012 finite elements. The results of the analysis are presented in Figs.11, 12 as histories of contact force F and vertical velocity V. The contact force was determined on the slab, (F_s), at the posts, (F_p), and on the horizontal tube, (F_t). The displacement velocity, V, was analysed in the points marked in Fig.9 by A (curve 1) and B (curve 2). When the structure falls on the slab, a complex process of compression of the bottom plate between the falling massive containers and the stationary slab takes place, its complexity being determined by many factors, such as:

- geometrical and physical nonlinearity: a significant value of the initial kinetic energy (49.5 kJ for the region analysed) predetermines the occurrence of plastic strains, large displacements and distortions;
- contact interaction between individual structural elements: the contact zone is multiply connected and localised in comparatively small regions of the structure surface, such as vertical post ends - slab, horizontal tube for a loader - slab, bottom plate frame - containers.

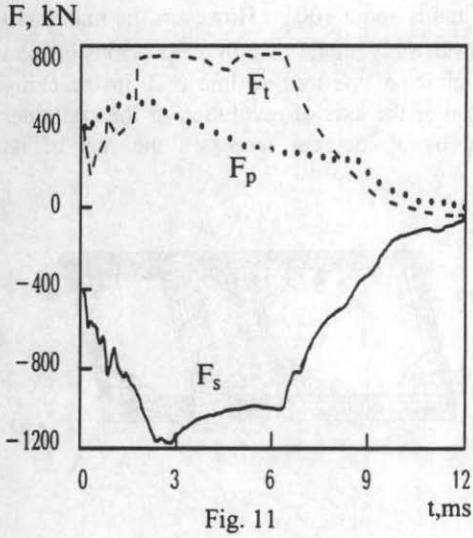

Fig. 11

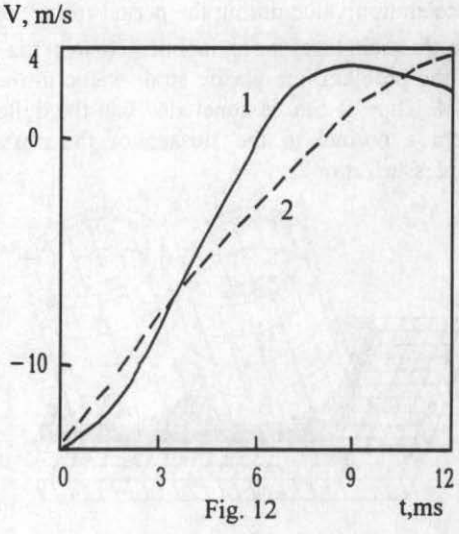

Fig. 12

As the side container interacts only with a part of the upper end surface of the post, the latter is compressed nonsymmetrically, which is accompanied by the appearance of a bending moment. When it reaches its critical value (at about t=1.5 ms) the posts become unstable and bend outside. As the kinetic energy of the containers at that time is rather high (35-40 kJ), the

bending is accompanied by intensive development of plastic strains. It should be noted that the steel tubes used as posts have rather thick walls. For thinner tube walls, the loss of stability could occur with the formation of local circumferential folds, both axisymmetrical and non-axisymmetrical.

Dynamic bending in the horizontal tube takes place both in the longitudinal and cross-sectional directions, the distortion of the tube cross-section significantly depending on its situation. Thus, in the middle part of the tube, its horizontal displacement is not confined by anything, the tube cross-section finally becoming oval. Meanwhile, at t=1.5 ms, at the ends, where the tube is attached to the bottom plate frame, loss of stability of the tube cross-section occurs, with a region buckling outside in the positive direction of the Z-axis. This is explained by the fact that the upper half of the tube is confined at the ends by the vertical walls of the frame.

Deformation of the supports leads to changes in the contact pressure field. Thus, at t=0.1 ms, the ratio of the contact force at the posts, F_p, (Fig.11) and that at the tube, F_t, is approximately 1.7. The weakening of the vertical posts due to the loss of stability leads to a smooth decrease in the integral contact force, F_p, in the "post-slab" zone. Under the effect of the outer container, the force at the posts is redistributed onto the horizontal tube, and at t>2 ms F_p is as low as 50-30% of F_t. Changes in the F_p/F_t relation are also reflected in the curve of the vertical velocity component, V(t) (Fig.12). After 2 ms, overload $\Delta V/\Delta t$ at the inner container situated over the horizontal tube is about 270 $\bar{g}$, and at the outer one (curve 2) is 180 $\bar{g}$.

Under the effect of the reaction forces, the bottom plate frame bends dynamically, acquiring the form corresponding to the contact force values at the supports. The analysis of the velocity field distribution reveals that at the initial stage (t<1.5 ms) the bending geometry of the bottom plate frame is determined mainly by the deceleration at the posts. After 3 ms, the frame continues to bend, being supported mainly by the horizontal tube. The strain distribution analysis at the bottom plate frame showed that maximum plastic strains are located at the vertical posts and the ends of the tubular rails for a loader. By t=9 ms, the plastic strains at the vertical posts reach the value of 47%, so the structure could be expected to fail at this location. However, at t>3 ms the supporting function of the posts reduces significantly, the main load being shifted onto the horizontal tube. At the ends of the horizontal tube, strains do not exceed 28%. Actually, cracking is also possible here, but it does not influence much the movement of the containers. This is due to the fact that excess of the limiting values (25%) takes place in the time interval t>6 ms, when the kinetic energy of the containers and the bottom plate is only 3% of the initial value.

If the bottom plate frame is initially perpendicular to the slab surface, the loads on the container-bottom plate attachment units increase on the impact, and the assessment of their strength becomes vital. The analysis reveals that in the above case the average value of overload $\Delta V/\Delta t$ during the first millisecond is 350-450 $\bar{g}$, its maximum value reaching 950 $\bar{g}$. Even if multiplied by the container mass, the overload value of 350 $\bar{g}$ gives the force equal to 850 kN, which considerably exceeds the allowable force for the bolts used.

CONCLUSION

A 3-D deformation problem of a container situated on a stationary base when struck by a solid slab was analysed. Both the height from which the slab falls and the orientation of the container in space were varied in the numerical experiments. The obtained results made it possible to determine the contact forces acting on the container, the overloads on the specimens situated inside the container, to locate the maximum strain zones and to evaluate them. The comparison of the results revealed the most hazardous situations for the above structure. Thus, it was found that displacement of the container off its vertical position increases the risk of its depressurization. A complex nonstationary deformation process of the bottom plate and the containers falling onto a rigid slab was analysed. The overloads on the containers were determined and the strength of the container-bottom plate attachment units was evaluated. The validity of the results is verified by their convergence analysis for a refined FE-mesh. Variation of the total energy of the structures analysed did not exceed 5%, which also testifies to a reasonable accuracy of the analysis.

The engineering experience shows that the numerical experiments based on the "DINAMIKA-3" software complex are 1 to 2 orders cheaper than the realistic tests, and in a number of cases the latter are absolutely prohibitive for the reasons of ecological safety. The use of the analyses not only allows one to gain a better insight into the processes studied, but also to develop the guidelines for improving the quality of the structures designed. In particular, interesting results are obtained in analysing the deformation of stand with containers in emergency situations possible when the latter are moved down the mine. The FE-analysis revealed that the shelf posts buckle elastoplastically on the impact with the bottom of the mine. As the gap between the mine walls and the posts is small, the extraction of the stand can be complicated. After a series of analyses a cross-section of the posts was determined allowing one to keep their bending in the acceptable limits. Unfortunately, these and many other results could not be included in the paper due to its limited volume.

The work was financially backed by Russian Fund of Fundamental Research under the Program for supporting the leading scientific schools of Russia, Grant # 96-15-98156.

REFERENCES

Bazhenov V.G., Kibetz A.I. Numerically modelling 3-D problems of nonstationary deformation of elastoplastic structures using FEM. Proc. Russian Academy of Sciences. Solid State Mechanics. 1994. No1. PP.52-57.

Bazhenov V.G. et al. Numerically modelling the nonstationary impact interaction processes in deformable structural elements. Problems of Engineering and Safety. 1995. No2. PP.20-26.